Title: Distinct representational structure and localization for visual encoding and recall during visual imagery

Authors: Wilma A. Bainbridge (1,2), Elizabeth H. Hall (3,2), Chris I. Baker (2)

Affiliations:

1 – Department of Psychology, University of Chicago; Chicago, IL 60637

2 – Laboratory of Brain and Cognition, National Institute of Mental Health; Bethesda, MD 20814

3 – Department of Psychology, University of California Davis; Davis, CA 95616

Corresponding Author: Wilma A. Bainbridge, wilma@uchicago.edu, (773)-702-3189

5848 S University Ave, Beecher Hall 303, Chicago, IL 60637

Running title: Distinct representations for encoding and recall

Abstract

During memory recall and visual imagery, reinstatement is thought to occur as an echoing of the neural patterns during encoding. However, the precise information represented in these recall traces is relatively unknown, with previous work investigating broad distinctions (scenes versus objects) or individual images, rarely bridging these levels of information. Using ultra-high-field (7T) fMRI with an item-based visual recall task, we conducted an in-depth comparison of encoding and recall along a spectrum of granularity, from broad stimulus class (scenes, objects) to object or scene type (natural, manmade) to individual categories (living room, cupcake). In the scanner, participants viewed a trial-unique item, and after a distractor task, visually imagined the initial item. During encoding, we observed decodable information at all levels of granularity in category-selective visual cortex, while during recall, only stimulus class was decodable. A closer look revealed a segregation between those voxels showing the strongest effects during encoding and those during visual recall. Finally, in a whole-brain analysis, we find peaks of encoding-recall similarity in regions anterior to category-selective cortex. Collectively, these results suggest visual recall is not merely a reactivation of encoding patterns, displaying a different granularity of information and localization from encoding, despite some overlap.

Keywords: 7T fMRI, encoding-recall similarity, objects, representational similarity analyses, scenes

Introduction

When we visually recall an object or scene, our memory contains rich object and spatial information (Bainbridge et al., 2019). During such recollection, our brain is thought to reinstate neural patterns elicited by the initial perception (McClelland et al., 1995; Buckner and Wheeler, 2001; Tompary et al., 2016; Dijkstra et al., 2019). One common view is that the hippocampus indexes populations of neocortical neurons associated with that memory (Teyler and Rudy, 2007; Danker and Anderson, 2010; Schultz et al., 2019). Under this view, representations in hippocampus are largely independent of a memory's perceptual content (Davachi, 2006; Liang et al., 2013; Huffman and Stark, 2014). In contrast, the neocortex is thought to show sensory reinstatement, where the same regions show the same representations during recall as during encoding (Wheeler et al., 2000; Kahn et al., 2004; Staresina et al., 2012; Ritchey et al., 2013; Lee et al., 2012; O'Craven and Kanwisher, 2000; Dijkstra et al., 2017). However, previous work looking at decodable information during recall has mainly focused on the broad stimulus class (Polyn et al., 2005; Johnson et al., 2009; Reddy et al., 2010; LaRocque et al., 2013) or traces for individual exemplars (Dickerson et al., 2007; Buchsbaum et al., 2012; Lee et al., 2012; Kuhl and Chun, 2014). The extent to which representations during recall reflect the same information as during perception, at all its levels of granularity (from individual exemplar up to broad stimulus class), is unclear. Here, using ultra-high-field (7T) fMRI, we conducted an in-depth investigation of the content of encoded and recalled representations of objects and scenes across cortex and hippocampus, assessing the granularity of detail in the representations of individual items.

First, we employed a hierarchically organized stimulus set (Figure 1) with three levels of granularity from broad stimulus class (scenes/objects) to stimulus type (e.g., natural/manmade

scenes) to individual items (e.g., bedrooms/conference rooms). Prior work comparing encoding and recall have primarily investigated memory content at opposite ends of this granularity spectrum. At a broad level, recall of stimulus classes (faces, scenes, objects) have been reported to reactivate high-level visual regions (Polyn et al., 2005; Johnson et al., 2009; Reddy et al., 2010; LaRocque et al., 2013) and produce differentiable responses in hippocampus (Ross et al, 2018). At a finer level, other work has shown reinstatement at the individual image or exemplar level, with specific items decodable in neocortical regions (Dickerson et al., 2007; Buchsbaum et al., 2012; Lee et al., 2012; Kuhl and Chun, 2014) and hippocampus (Zeineh et al., 2003; Gelbard-Sagiv et al., 2008; Chadwick et al., 2010; Wing et al., 2015; Mack and Preston, 2016; Tompary et al., 2016; Lee et al., 2019). However, it is unclear what information drives discrimination, whether it is low-level visual content, perceptual categories, or memory strength. For example, while recalled grating orientation is decodable from early visual cortex (V1-V3), reinstatement strength but not content is decodable from the hippocampus (Bosch et al., 2014). Our approach using nested levels of stimulus information reveals what granularity of information is contained in these regions, and whether reinstatement is simply an echo of the same response from encoding to recall.

Second, to isolate the activity specific to recall, we adopted a visual imagery task focusing on recall of individual items without requiring the learning of cue-stimulus associations, which have commonly been used (e.g., Ganis et al., 2004; Kuhl et al., 2012; Zeidman et al., 2015a; Jonker et al., 2018). Recalled representations in associative tasks are likely to contain information not only about the recalled item, but also the cue and the association itself. Further, there are differences in neocortex when performing an associative versus item-based memory

task (Staresina and Davachi, 2006). In fact, the neural representation of a target may be largely dependent on what cue it is associated with (Xiao et al., 2017). Here, we employ an item-based recall task in which participants encode trial-unique images, and following a distractor task, recall that specific image. This approach allows us to investigate the recall of individual items, without the learning of associations.

Using this direct recall task and nested stimulus structure, we find striking differences in the representational structure and spatial localization for visual encoding and recall, suggesting recall patterns are not just a repetition of patterns during encoding, despite some similarities.

Materials and Methods

Participants

Thirty-four adults were recruited for the experiment. All participants were healthy, right-handed, and had corrected or normal vision. Twelve participants were unable to complete the experiment due to discomfort in the 7T scanner or scanner malfunction, and their data were excluded from the study. This level of participant dropout is not unusual for 7T scans, given that nausea and vertigo occasionally occur, and the bore is more restrictive than the more standard 3T scanners. The final set of participants included twenty-two adults (fifteen female). All participants provided consent following the guidelines of the National Institutes of Health (NIH) Institutional Review Board (ZIA-MH-002909, National Institute of Mental Health Clinical Study Protocol NCT00001360, 93M-0170), and were compensated for their participation.

Stimuli

Stimulus images comprised 192 images, 50% objects and 50% scenes, with nested categorical structure (Figure 1a). The objects were made up of four object types, varying along two factors known to show differential responses in the brain during perception: 1) small / big objects (Konkle et al., 2012), and 2) tool / non-tool objects (Valyear et al., 2007; Mahon et al., 2007; Beauchamp and Martin, 2007). Small versus big object categories were defined based on prior literature (Konkle et al., 2012; Bainbridge et al., 2015). Tools were defined as objects commonly grasped by one's hands using a power grip (e.g., Grèzes et al., 2003), although note that there are multiple ways tools are defined in the field (Lewis, 2006). The other half of the stimulus images were scenes, varying along two factors shown to elicit differential responses in the brain: 1) natural / manmade (Park et al., 2011), and 2) open / closed (Kravitz et al., 2011). Each object or scene type contained three categories, with eight exemplars for each object or scene category (e.g., <u>small, non-tool objects</u>: bowl, cupcake, flowers; <u>closed, manmade scenes</u>: bathroom, conference hall, living room). Note that for clarity, we will refer to the most fine-grained level of categorization (e.g., cupcake, bathroom) as stimulus *category*, the mid-level of categorization (e.g., big/small objects, open/closed scenes) as stimulus *type*, and the distinction of objects versus scenes as stimulus *class*. Images were all square 512 x 512 pixel images presented at 8 degrees visual angle, and objects were presented cropped in isolation on a white background.

a)

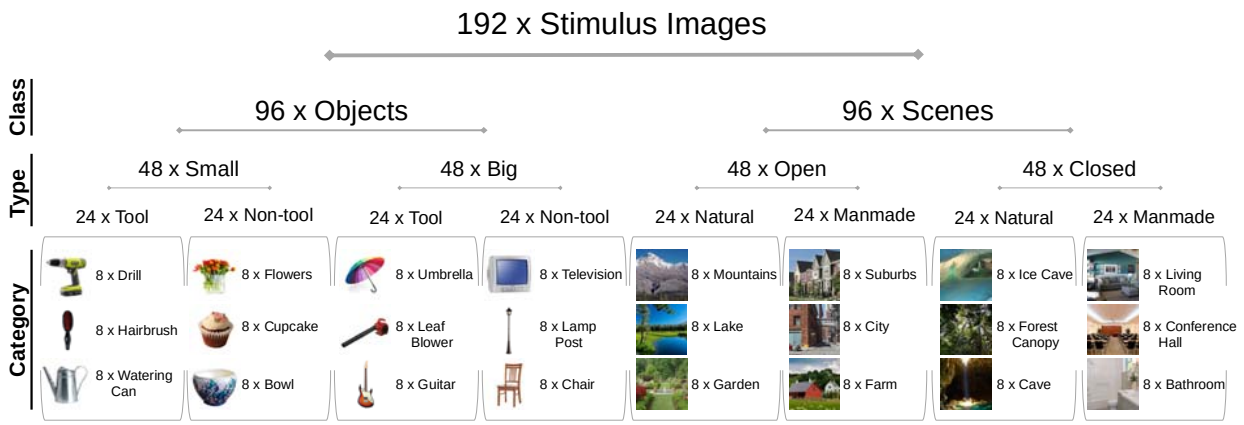

b)

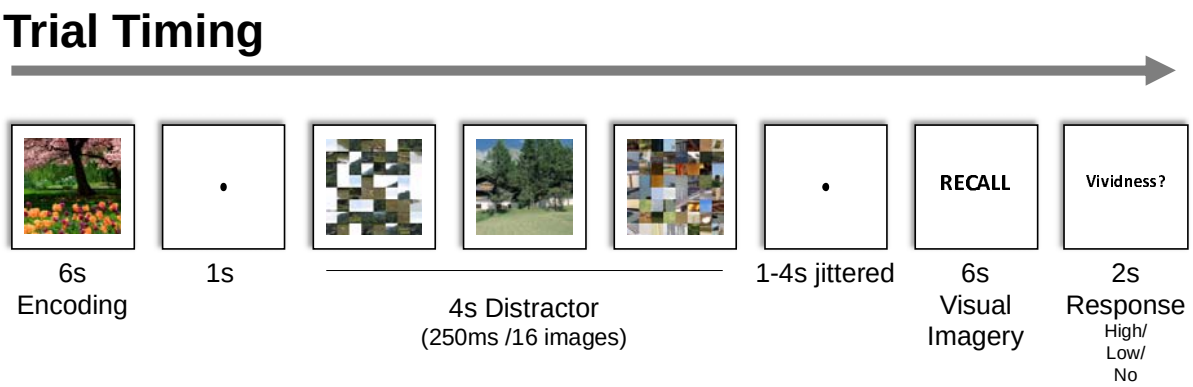

Figure 1. Experimental stimuli and task. (a) Nested structure of stimuli and example images. 192 trial-unique images were encoded and recalled by participants, arranged under nested structure based on broad stimulus *class* (object / scene), stimulus *type* (e.g., open / closed or natural / manmade scene), and stimulus *category* (mountains / lake). Each stimulus category contained 8 different exemplar images (e.g., 8 different lake photographs). (b) The timing of each trial. Participants studied an image for 6 s, performed a distractor task requiring detection of an intact image amongst scrambled images for 4 s, and then after a randomized jitter of 1-4 s, recalled the original image through visual imagery for 6 s. Finally, they indicated the vividness of their memory with a button press.

In-scanner recall task and post-scan recognition task

Participants first completed a single run of a 7-min 6-sec block-design localizer scan to identify scene- and object-selective regions. In this localizer, participants viewed blocks of images of objects, scenes, faces, and mosaic-scrambled scenes and identified consecutive repeated images. All images used in the localizer were distinct from those used in the main experiment. Participants then completed eight runs of an item-based memory recall task requiring visual imagery (Figure 1b). In each trial, participants studied a trial-unique stimulus image for 6 s. After a 1 s fixation, they performed a distractor task in which they viewed a stream of 16 quickly presented images (250 ms each), and had to press a button as soon as they saw the sole intact image in a stream of mosaic-scrambled images. Scrambled and intact target images were taken from a separate stimulus set, and were chosen to be of the same broader stimulus class (i.e., object or scene) as the studied image, but of random type and category. Intact object images were presented as an intact object against a mosaic-scrambled background, so that participants would have to fixate the object to successfully perform the task (rather than identify white edges). The distractor task lasted for 4 s total and was followed by a 1-4 s jittered interval in which participants were instructed to wait and maintain fixation. The word "RECALL" then appeared on the screen for 6 s, and participants were instructed to silently visually imagine the originally studied image in as much detail as possible. Finally, following the "RECALL" phase, participants were given 2 s to press a button indicating the vividness of their memory as either no memory, low vividness, or high vividness. The next trial then continued after a 1 s delay. Participants were instructed that the task was difficult, and they should focus on reporting their vividness truthfully. Trials in which participants indicated "no memory" were not included in any analyses of the data, except for an analysis classifying response behavior

161 from brain patterns. However, no results meaningfully change when “no memory” are kept in
162 all analyses. Each run contained 24 trials, lasting 8 min 38 s, and participants completed 8 runs
163 total. Each run included three “catch trials” that skipped the recall phase, in order to keep
164 participants vigilant, to discourage them from pre-emptively recalling the target image, and to
165 better separate encoding from distractor and recall phases during deconvolution. Each stimulus
166 category (e.g., guitar, cupcake) was shown once per run, and each stimulus exemplar image
167 was only used once in the entire experiment, so that there would be no memory effects on
168 subsequent presentations of the same image.

169 After the scan, participants performed a post-scan recognition task to test their memory
170 for the images studied in the scanner. Participants were presented with all 192 images studied
171 in the scanner randomly intermixed with 192 foil images of the same stimulus categories and
172 were asked to indicate for each image whether it was old or new. Two participants were unable
173 to complete the post-scan recognition task due to time constraints.

174

175 *MRI acquisition and preprocessing*

176 The experiment was conducted at the NIH, using a 7T Siemens MRI scanner and 32-
177 channel head coil. Whole-brain anatomical scans were acquired using the MP2RAGE sequence,
178 with 0.7 mm isotropic voxels. Whole-brain functional scans were acquired with a multiband EPI
179 scan of in-plane resolution 1.2 x 1.2 mm and 81 slices of 1.2 mm thickness (multiband factor=3,
180 repetition time=2 s, echo time=27 ms, matrix size=160 × 160, field of view=1728 × 1728, flip
181 angle=55 degrees). Slices were aligned parallel with the hippocampus and generally covered
182 the whole brain (when they did not, sensorimotor parietal cortices were not included).

183 Functional scans were preprocessed with slice timing correction and motion correction using
184 AFNI and surface-based analyses were performed using SUMA (Cox, 1996; Saad and Reynolds,
185 2012).
186
187 *FMRI Region of Interest (ROI) Definitions*
188 Key ROIs for early visual cortex, object selective cortex, scene selective cortex, and
189 hippocampus were determined *a priori* and defined using functional and anatomical criteria
190 (Figures 3 and 4). Using the independent functional localizer, we identified three scene-
191 selective regions with a univariate contrast of scenes > objects: PPA (Epstein & Kanwisher,
192 1998), medial place area (MPA; Silson et al., 2016), and occipital place area (OPA; Dilks et al.,
193 2013). We localized object-selective regions lateral occipital (LO) and posterior fusiform (pFs)
194 with a univariate contrast of objects > scrambled images (Grill-Spector et al., 2001). Finally, we
195 localized early visual cortex (EVC) with a univariate contrast of scrambled images > baseline.
196 The ROIs were based on activation within areas defined by the literature (e.g., Epstein and
197 Kanwisher, 1998; Grill-Spector et al., 2001), and were selected first at a threshold of False
198 Discovery Rate (FDR)-corrected threshold of $q = 0.01$, and then selection criteria were gradually
199 relaxed (up to p=0.05) until any voxels in that area were found. Left and right ROIs were
200 combined to create bilateral ROIs. Overlapping voxels between scene- and object-selective
201 regions were discarded. LO, pFs, PPA, and EVC were identified bilaterally in 22 participants, OPA
202 in 21 participants (20 bilateral), and MPA in 20 participants (17 bilateral). Anatomical ROIs were
203 localized using FreeSurfer's recon-all function using the hippocampal-subfields-T1 flag (Iglesias
204 et al., 2015), and then visually inspected for accuracy. This hippocampus parcellation function

splits the hippocampus into the head/body (Hip-HB) and tail (Hip-T), and within the head/body region further segments the hippocampus into different subfields (dentate gyrus, CA1, CA3, and subiculum; Iglesias et al., 2015). We did not find meaningful differences across subfields, but report those results in the Supplementary Information. For the main body of the text, we report the results from the Hip-HB (with subfields combined) and Hip-T. We also looked at medial temporal lobe regions perirhinal cortex and parahippocampal cortex (outputted by the same automatic segmentation pipeline), and include those results in the Supplementary Information.

Whole-Brain Univariate Analyses

We conducted whole-brain univariate contrasts using a generalized linear model (GLM) that split the trials into four regressors along two factors: 1) encoding / recall, and 2) scenes / objects. Six additional regressors for movement were also included. Trials in which participants indicated they had “no memory” for the item were not included in the GLM. We then performed whole-brain T-contrasts of scenes vs. objects separately during encoding and recall. All whole-brain images were projected onto the cortical surface using AFNI surface mapper SUMA (Saad and Reynolds, 2012).

Representational Similarity Analyses and Discrimination Indices

Multivariate analyses were conducted to look at the representations of different stimulus information during encoding and recall, across brain regions. For these analyses, the experimental data were first split into two independent halves – even runs and odd runs. For each split half, a GLM was calculated, modeling separate regressors for each stimulus category

227 (e.g., cupcake) for the encoding period (6 s boxcar function), distractor period (4 s boxcar), and
228 recall period (6 s boxcar). Each event (e.g., encoding a cupcake) thus had two resulting beta
229 estimates: one across even runs, and one across odd runs. Trials in which participants indicated
230 they had no memory for the image (M=9.31% of trials per participant, SD=8.38%, Min=0%,
231 Max=35.16%, Median=6.46%) were not included in the GLMs. The estimated motion
232 parameters from the motion correction were included as six additional regressors.

233 We then investigated the similarity between different types of stimulus information
234 during both encoding and recall, using representational similarity analyses (RSA; Kriegeskorte et
235 al., 2008). For each ROI, we created a representational similarity matrix (RSM) comparing the
236 similarity of all pairs of stimulus category (e.g., cupcake vs. guitar). Similarity was calculated as
237 the Pearson's correlation between the voxel values (t-statistic) in an ROI for one category (e.g.,
238 cupcake) from one half of the runs (e.g., odd runs), with the voxel values for another category
239 (e.g., guitar) from the other half (e.g., even runs). Specifically, pairwise item similarity was taken
240 as the average of the correlation with one split (odd runs for item A, even runs for item B) and
241 correlation with the opposite split (even runs for item A, odd runs for item B). This metric
242 indicates the similarity in the neural representations of two categories, and importantly,
243 because the comparisons use separate halves of the data, we can observe a category's
244 similarity to itself across runs. This self-similarity measure thus shows the degree to which a
245 given region shows similarity across exemplars within category (i.e., are cupcakes similar to
246 other cupcakes). These similarity matrices were created in three ways: 1) correlations of the
247 encoding trials (Encoding RSM), 2) correlations of the recall trials (Recall RSM), 3) correlations
248 of the encoding trials with the recall trials (Cross-Discrimination RSM). These different

classifications allow us to see what stimulus information exists separately during encoding and recall, as well as what information is shared between encoding and recall.

From these RSMs, we conducted discriminability analyses, which show the degree to which each ROI can discriminate the different conditions of class, type, and category (e.g., do the responses in PPA discriminate natural vs. manmade scenes?). For each comparison of interest, we computed a discriminability index *D,* calculated as the difference of the mean across-condition correlations (e.g., scenes with objects) from mean within-condition correlations (e.g., scenes with other scenes; Kravitz et al., 2011; Cichy et al., 2014; Harel et al., 2013; Harel et al., 2014; Henriksson et al., 2015). The intuition behind this index is that if an ROI contains information about that comparison, then within-condition similarity should be higher than across-condition similarity (e.g., if the PPA *does* discriminate natural vs. manmade scenes, then natural scenes should be more similar to other natural scenes than manmade scenes). Significant discriminability was determined by a two-tailed t-test comparing discrimination indices across participants versus a null result of 0. Type discriminability was only computed within same-class items (e.g., only scenes were used for the natural vs. manmade comparison), and category discriminability was only computed within same-type items (e.g., when looking at the discriminability of living rooms, they were only compared to other closed, manmade scenes). For the encoding and recall discrimination indices, all statistics reported are FDR-corrected within each ROI at a value of $q < 0.05$ unless noted otherwise. Refer to Figure 2 for a depiction of these discrimination indices and to see example RSMs.

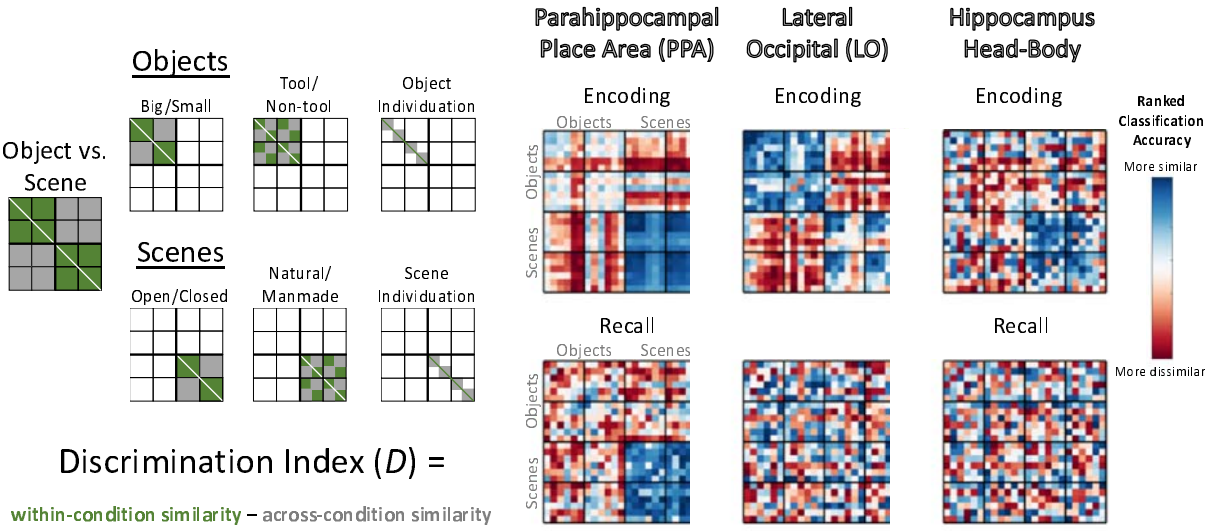

Figure 2 – Calculating information discriminability from representational similarity matrices. (Left) Depictions of the cells of the representational dissimilarity matrices (RSMs) used to calculate discrimination indices for key regions of interest (ROIs). The RSMs represent pairwise Pearson's correlations of stimulus groupings calculated from ROI voxel t-values, compared across separate run split halves (odd versus even runs). These depictions show which cells in the matrices are used in the calculation of discriminability of different properties, with green cells indicating within-condition comparisons, which are compared with grey cells indicating across-condition comparisons. For all discriminability calculations except discrimination of individual categories (i.e., individuation), the diagonal was not included. All operations were conducted on the lower triangle of the matrix, although both sides of the diagonal are shown here for clarity. (Right) Examples of encoding and recall RSMs from the data in the current study, specifically the rank-transformed average RSM for the parahippocampal place area (PPA), lateral occipital (LO), and the hippocampus head and body. Blue cells are more similar, while red cells are more dissimilar.

ROI-to-ROI similarity analysis

We investigated ROI-to-ROI correlations to assess similarity between ROI representations separately during encoding and recall. For each participant, we constructed an RSM for each ROI, as described in the previous section. We then constructed an ROI-to-ROI

similarity matrix by conducting secondary correlations between the RSMs for each pair of ROIs. Specifically, we correlated the ROI RSM calculated with half of the runs with the one created using the other half of the runs, so we could also look at an ROI's similarity to itself across runs and avoid any common fluctuations within runs (Henriksson et al., 2015). We additionally conducted multidimensional scaling (MDS), to visualize the similarity structure of these ROIs in two dimensions. This ROI-to-ROI similarity analysis was conducted separately for encoding trials and recall trials.

Discrimination-based Searchlight Analyses

We also conducted discriminability analyses using spherical searchlights (3-voxel radius) in two ways. First, we conducted discriminability analyses (as described above) for searchlights centered on voxels in the ROIs. For each searchlight, we obtained a scene-object discriminability metric during encoding and one during recall, allowing us to examine the relationship between encoding and recall information in these ROIs.

Second, we conducted discriminability analyses in searchlights iteratively moved through each individual's brain, to examine ability to discriminate information outside of our pre-defined ROIs. Group maps were combined with a two-tailed t-test comparing group discrimination indices versus no discrimination (0). Group maps were thresholded at $p < 0.01$ uncorrected for visualization purposes, however we also provide unthresholded maps. We conducted these searchlights looking at both discriminability of information within memory process type (encoding or recall), as well as ability to cross-discriminate (e.g., correlating encoding and recall patterns).

Modeling behavior

We conducted analyses to relate fMRI activity to behavioral measures of reported recall vividness and post-scan recognition performance. An additional GLM was conducted to obtain an estimate for each trial for each run, so that they could be compared with trial-by-trial behavior measures. In this case, no memory trials were not removed, so that we could look at ability to classify memory vividness responses. We employed support vector machines (SVMs) to classify recall vividness responses (no memory, low vividness, high vividness) from ROI patterns during encoding or recall. These SVMs were conducted on all pairs of the three classes, and then classification accuracies were averaged, although we also report the results of classifying just low versus high vividness trials. We also used SVMs to measure the ability to classify later successful recognition versus failed recognition (hits vs. misses) from ROI patterns during encoding or recall. All SVMs were conducted using a leave-one-run-out approach.

Results

In the following sections, we present several analyses elucidating the relationship between representations elicited during encoding and recall. First, we investigate what stimulus-based content can be discriminated from encoding and recall response patterns in object- and scene-selective visual ROIs and the hippocampus. Second, we calculate the degree to which these patterns can be used to decode memory strength and performance for individual items. Third, we analyze the relationships between these ROIs to see how they change during encoding and recall. Finally, we conduct searchlight analyses to investigate the

332 distribution of voxels showing the strongest discrimination during encoding, recall and between
333 these two phases, both within and outside the ROIs.
334
335 **Decoding stimulus content from scene- and object-selective visual regions and hippocampus**
336 What aspects of a visual memory are represented in scene- and object-selective areas
337 and hippocampus during encoding and recall? We asked this question by discriminating
338 stimulus information from the patterns of blood oxygen level dependent (BOLD) responses at
339 various scales of stimulus granularity, ranging from broad stimulus class (scenes, objects), to
340 stimulus type (e.g., natural/manmade scene, big/small object), to specific stimulus category
341 (e.g., cupcake, guitar). This discrimination was conducted across independent exemplars, never
342 including the same images in the training and testing sets of the decoding model. This allowed
343 us to see what levels of information are represented in these regions, separate from an ability
344 to distinguish identical images.
345
346 *Scene- and object-selective ROIs: Detailed information during encoding, limited information*
347 *during recall*
348 We investigated discriminability in object-selective regions LO and pFs and scene-
349 selective regions PPA, MPA, and OPA (Figure 3). Analyses for other regions including early visual
350 cortex, perirhinal cortex, and parahippocampal cortex (separate from the PPA) are reported in
351 the Supplementary Information. All object- and scene-selective regions could discriminate
352 broad stimulus class (objects vs. scenes) during encoding (LO: $t(21)=5.99$, $p=6.00 \times 10^{-6}$; pFs:
353 $t(21)=5.98$, $p=6.24 \times 10^{-6}$; PPA: $t(21)=7.08$, $p=5.50 \times 10^{-7}$; MPA: $t(19)=6.50$, $p=3.18 \times 10^{-6}$; OPA:

354 $t(20)=7.10$, $p=9.34 \times 10^{-7}$). Object type of tool/non-tool could be discriminated in object-
355 selective regions LO ($t(21)=3.59$, $p=0.002$), and pFs ($t(21)=2.69$, $p=0.014$), and object size did not
356 show significant discriminability in any region. Individual object categories could be
357 discriminated in all regions except MPA (MPA: $p=0.085$; LO: $t(21)=5.22$, $p=3.61 \times 10^{-5}$; pFs:
358 $t(21)=5.29$, $p=3.00 \times 10^{-5}$; PPA: $t(21)=4.10$, $p=5.10 \times 10^{-4}$; OPA: $t(19)=4.44$, $p=2.80 \times 10^{-4}$). Scene
359 types could also be decoded from most regions, including open/closed (LO: $t(21)=4.37$, $p=2.70 \times$
360 10^{-4}; pFs: $t(21)=3.32$, $p=0.003$; PPA: $t(21)=4.08$, $p=5.36 \times 10^{-4}$) and natural/manmade (LO:
361 $t(21)=4.29$, $p=3.26 \times 10^{-4}$; pFs: $t(21)=3.13$, $p=0.005$; PPA: $t(21)=3.65$, $p=0.001$; MPA: $t(19)=4.16$,
362 $p=5.33 \times 10^{-4}$). Finally, individual scene categories could also be discriminated in scene-selective
363 regions PPA ($t(21)=3.60$, $p=0.002$) and OPA ($t(20)=3.55$, $p=0.002$). Overall, these results
364 confirmed the findings of prior studies (e.g., Valyear et al., 2007; Walther et al., 2009; Park et al.,
365 2011; Kravitz et al., 2011; Troiani et al., 2012), in which responses in scene- and object-selective
366 regions can be used to distinguish various levels of information about visually presented scenes
367 and objects.

368 During recall, all high-level visual regions could distinguish recalled objects from scenes
369 (LO: $t(21)=3.44$, $p=0.002$; pFs: $t(21)=2.66$, $p=0.015$; PPA: $t(21)=4.27$, $p=3.40 \times 10^{-4}$; OPA:
370 $t(20)=3.31$, $p=0.004$), although MPA did not pass FDR correction (MPA: $t(19)=2.54$, $p=0.020$). No
371 region showed significant discriminability for object type (big/small, tool/non-tool) nor scene
372 type (open/closed, natural/manmade) during recall. No region showed discrimination of object
373 category nor scene category. We also compared stimulus discriminability between encoding
374 and recall for the cases in which there was significant information during encoding. For all ROIs,
375 encoding showed significantly higher discriminability of stimulus class than recall (all $p < 0.001$).

For stimulus type, encoding discriminability was again significantly higher than recall discriminability for all ROIs and comparisons, except a marginal difference for tool discriminability in LO ($t(21)=1.99$, $p = 0.058$). Finally, for stimulus category, PPA showed no significant difference between encoding and recall for object individuation ($p = 0.053$) and scene individuation ($p = 0.295$). Similarly, OPA did not show a significant difference for scene individuation ($p = 0.286$). This indicates that encoding and recall discriminability of individual categories may be at similar levels in these regions. However, pFs and LO show significantly higher discriminability of object category during encoding compared to recall (both $p < 0.005$). Overall, these results reveal that while multiple regions maintain information about broad stimulus class during recall, and there may be some evidence for similar levels of information between encoding and recall for fine-grained stimulus category, we find no evidence for decoding intermediate stimulus information during recall.

To investigate which regions show a shared neural representation during encoding and recall, we conducted a cross-discrimination analysis identifying the degree to which a region shows similar patterns between encoding and recall. The only significant cross-discrimination was for stimulus class (objects versus scenes), which was found in pFs ($t(21)=2.94$, $p=0.008$), PPA ($t(21)=2.83$, $p=0.010$), and MPA ($t(19)=3.99$, $p=7.89 \times 10^{-4}$). Significant cross-discrimination did not emerge for any finer-grained stimulus information in scene- and object-selective ROIs.

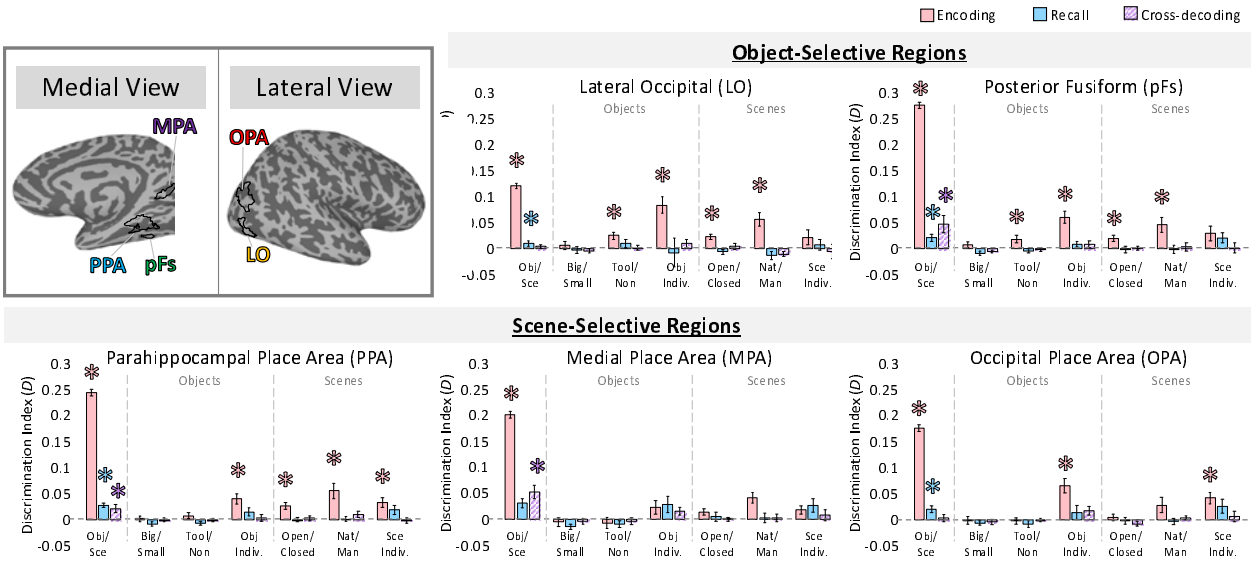

Figure 3 – Information discriminability in scene- and object-selective regions. Discriminability for scene- and object-selective regions of interest (ROIs) for each stimulus property was calculated from the RSMs (as in Figure 2). ROIs correspond to those shown in the upper left; shown here are probabilistic ROIs chosen as voxels shared by at least 12% participants, however analyses were conducted in individually localized ROIs. Bar graphs indicate mean discrimination index for different comparisons across ROIs, are split by broad stimulus class, and show three levels of discrimination: 1) broad discrimination of stimulus *class* (objects versus scenes), 2) mid-level discrimination of stimulus *type* (objects: big/small, tools/non-tools; scenes: open/closed, natural/manmade), and 3) fine-grained discrimination of stimulus *category* (object and scene individuation). The y-axis represents the average discrimination index (*D*), which ranges from -1 to 1 and can be compared to a null level of 0. Pink bars indicate discriminability during encoding trials, blue bars indicate discriminability during recall trials, and hatched purple bars indicate cross-discriminability (i.e., there is a shared representation between encoding and recall). Error bars indicate standard error of the mean. Asterisks (*) indicate significance at a FDR corrected level of $q<0.05$.

Hippocampus Shows Stimulus Class Information During Encoding

We conducted the same analyses in hippocampal ROIs (Figure 4). During encoding, the Hip-HB showed significant discrimination of objects versus scenes ($t(21)=4.16$, $p=4.44 \times 10^{-4}$) However, the Hip-HB showed significant sensitivity to no other information during encoding.

Interestingly, this pattern in the Hip-HB during encoding was similar to the scene- and object-selective visual areas during recall, in their specific ability to discriminate broad stimulus class. The Hip-T showed no significant discriminability at any level during encoding. During recall, neither hippocampal region showed significant discriminability of any level of information ($q > 0.05$), and was significantly lower than encoding discriminability for stimulus class ($t(21)=3.84$, $p=9.42 \times 10^{-4}$). No significant cross-discrimination between encoding and recall was observed ($q > 0.05$). No meaningful differences were found when looking at individual hippocampal subfields (Supplementary Information). Overall, the only information that emerged in the hippocampus was a difference between objects and scenes during encoding, and we found no evidence for discriminability of intermediate information during encoding, nor any level of information during recall.

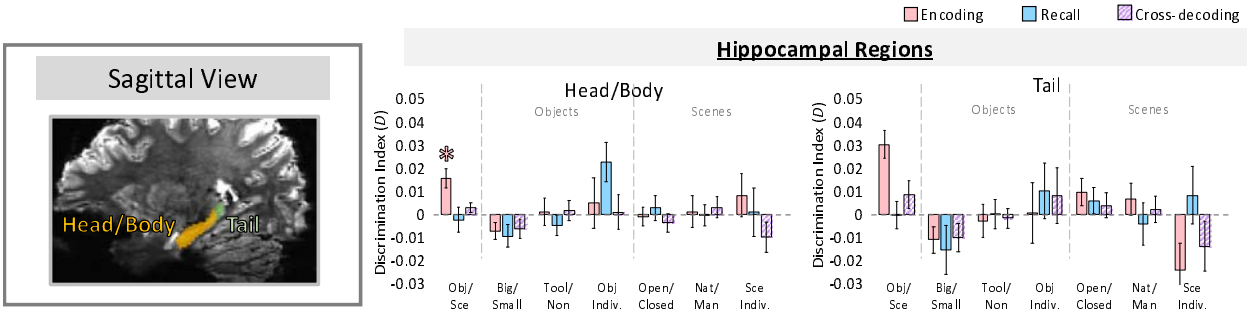

Figure 4 – Information discriminability in the hippocampus. Discriminability for hippocampal ROIs of each stimulus property was calculated from the RSMs. On the left is an example participant's 7T functional scan overlaid with their automatically segmented hippocampal regions (head/body and tail). Bar graphs are displayed in the same manner as Figure 3, and indicate mean discrimination index for comparisons of different levels of stimulus information (class, type, and category for objects and scenes). Pink bars indicate discriminability during encoding trials, blue bars indicate discriminability during recall trials, and hatched purple bars indicate cross-discriminability

(i.e., there is a shared representation between encoding and recall). Error bars indicate standard error of the mean. Asterisks (*) indicate significance at a FDR corrected level of $q<0.05$.

Relationship of fMRI response patterns to memory behavior

In contrast to the specific visual content of a stimulus, to what degree do these regions represent information about the strength of the memory? We examined the ability to use the voxel values in each region to decode participant-reported memory vividness, a rating provided by participants after each recall trial in the scanner (Figure 5a). We also examined the ability to decode recognition success for each image based on a post-scan old/new recognition task (Figure 5b).

FMRI response patterns and memory vividness

On average, participants reported 'high vividness' on 60.8% of trials (SD=16.9%), 'low vividness' on 29.9% of trials (SD=12.8%), and 'no memory' on 9.31% of trials (SD=8.38%). We tested the ability to classify this memory vividness from patterns in the different ROIs during encoding and recall. In only this analysis, we included trials rated as "no memory" in the classifier. Encoding patterns from all scene- and object-selective regions were predictive of recall vividness: LO (M=62.28%, $t(21)=5.43$, $p=3.09 \times 10^{-5}$), pFs (M=60.90%, $t(21)=4.90$, $p=9.99 \times 10^{-5}$), PPA (M=57.11%, $t(20)=4.99$, $p=8.12 \times 10^{-5}$), MPA (M=55.72%, $t(19)=2.40$, $p=0.027$), and OPA (M=57.51, $t(20)=4.31$, $p=4.20 \times 10^{-4}$). In contrast, within the hippocampus, (Hip-HB and Hip-T), encoding patterns could not be used to classify recall vividness (both $p>0.05$). Recall patterns from all scene- and object-selective regions were also predictive of recall vividness: LO

455 (M=56.43%, $t(21)=4.22$, $p=4.61 \times 10^{-4}$), pFs (M=55.83%, $t(21)=3.36$, $p=0.003$), PPA (M=55.63%,
456 $t(19)=2.63$, $p=0.016$), MPA (M=57.50%, $t(19)=3.06$, $p=0.007$), and OPA (M=58.26%, $t(20)=3.85$,
457 $p=0.0012$). Additionally, the hippocampus showed memory vividness decodability from
458 patterns during recall, in both the Hip HB (M=53.34%, $t(21)=2.76$, $p=0.012$) and Hip T
459 (M=54.26%, $t(21)=2.49$, $p=0.022$). While hippocampus showed decodability during recall and
460 not during encoding, there was no significant difference in classification accuracy between
461 encoding and recall (both regions: $p>0.05$).

462 If we look specifically at the ability to classify low vividness from high vividness trials, a
463 subset of these ROIs shows above-chance classification accuracy. Specifically, during memory
464 encoding, patterns in the pFs (M=62.35%, $t(21)=2.82$, $p=0.013$) and OPA (M=58.70%, $t(20)=4.90$,
465 $p=2.33 \times 10^{-4}$) can differentiate low and high vividness trials. During recall, pFs (M=57.22%,
466 $t(21)=2.15$, $p=0.048$), PPA (M=61.07%, $t(19)=2.85$, $p=0.012$) , and OPA (M=59.20%, $t(20)=2.19$,
467 $p=0.046$) patterns can differentiate low vividness from high vividness trials. The hippocampus
468 did not show ability to differentiate low vividness or high vividness trials during encoding nor
469 recall (both regions: $p>0.10$).

470 These results indicate that scene- and object-selective regions contain information
471 about memory vividness during both encoding and recall. In contrast, the hippocampus only
472 contains information about memory vividness during the recall period, when classifying all trial
473 types (high vivid, low vivid, and no memory). However, it is less clear whether the hippocampus
474 shows decoding of more fine-grained differences in vividness (differentiating high versus low
475 vividness).

476

FMRI response patterns and subsequent memory

Encoding patterns from scene- and object-selective regions were predictive of later successful recognition, from the LO (M=53.08%, $t(21)=2.31$, $p=0.032$), PPA (M=52.08%, $t(21)=2.29$, $p=0.033$), and OPA (M=53.35%, $t(21)=3.86$, $p=0.001$). MPA, pFs, Hip HB and Hip T did not show significant decodability of successful recognition (all $p>0.10$). No recall patterns from any ROI were predictive of later successful recognition (all $p>0.10$). These results confirm prior findings demonstrating an ability to predict subsequent memory performance from visual areas (Brewer et al., 1998), and show little ability to decode later recognition success from neural information during the recall period.

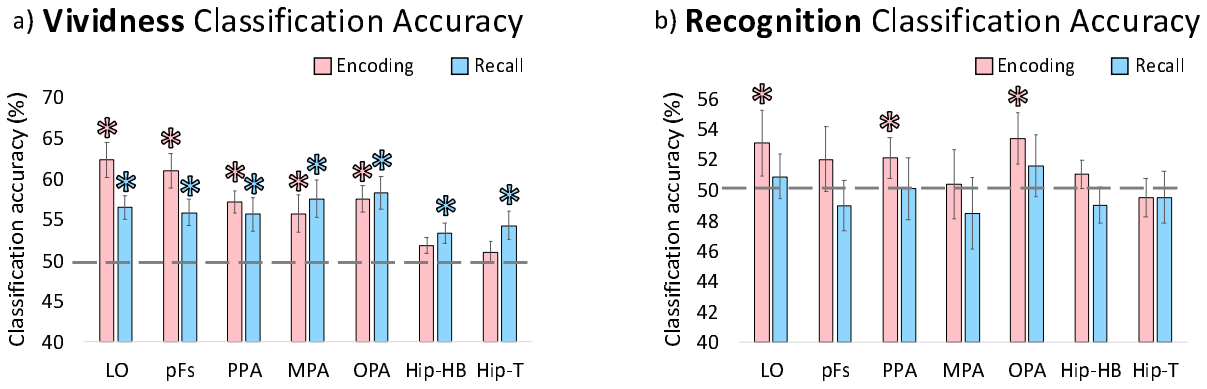

Figure 5 – Relationship of fMRI response patterns to behavior. (a) Classification accuracies for predicting subjectively reported recall vividness, based on patterns of encoding (pink) and recall (blue) from the ROIs. Chance level is 50%, and marked with the dashed grey line. Asterisks indicate a significantly higher classification accuracy than chance ($p < 0.05$). In scene- and object-selective visual regions, patterns during both encoding and recall can significantly predict the vividness of recall. In the hippocampus, only patterns during recall can significantly predict memory vividness. (b) Classification accuracies for predicting post-scan memory performance in a recognition task from patterns of encoding (pink) and recall (blue) from the ROIs. Only patterns from some scene- and object-

selective regions during encoding (LO, PPA, OPA) show significant ability to predict later recognition success. No patterns during recall were linked with recognition success.

Region-to-region similarity during encoding and recall

Beyond investigating the stimulus content representations within individual regions, an equally important question is how these visual and memory regions relate to each other in their representations during encoding and recall. While two regions may both contain information about a stimulus property, they may represent that information differently. The relationships between regions may also change meaningfully based on memory task (e.g., encoding versus recall). Thus, understanding the interactions among regions provides additional information on how stimulus representations are instantiated in the brain.

We looked at correlations of the RSMs between each pair of ROIs, separately for objects and scenes during both encoding and recall (Figure 6). These correlations were conducted using separate halves of the data, so diagonal values indicate an ROI's similarity to itself across runs of independent stimuli. We also conducted MDS to visualize the similarities across regions (Figure 6). For encoding objects and scenes, all regions were significantly self-correlated across runs (all $p < 0.001$), indicating that these regions show consistent patterns across runs and exemplars. Within the MDS for encoding both objects and scenes, scene- and object-selective regions are grouped together, with object regions LO and pFs similar to each other for object encoding, and scene regions PPA, MPA, OPA similar to each other for scene encoding. Meanwhile, hippocampal regions are highly dissimilar from all scene- and object-selective regions.

During recall, the representational structure of these regions transforms. All ROIs are still significantly correlated with themselves for recalling objects and scenes (all $p < 0.05$). However, scene- and object-selective regions are more dissimilar from each other, and these regions and hippocampus are more similar (Figure 6). To quantify cortical-hippocampal similarity, we compared the mean ranked correlation coefficient of the scene- and object-selective ROIs (pFs, LO, PPA, MPA, OPA) with the hippocampal ROIs (Hip-HB, Hip-T) between encoding and recall. In a 2-way ANOVA for stimulus class (object/scene) and memory process (encoding/recall), there was a significant difference in cortical-hippocampal similarity between encoding and recall ($F(1,84)=5.45$, $p=0.030$), but no main effect of stimulus category ($F(1,84)=0.002$, $p=0.961$) nor an interaction ($F(1,84)=0.76$, $p=0.394$). A post-hoc t-test indicated that cortical-hippocampal similarity was significantly higher during recall than encoding ($t(43) = 2.59$, $p=0.013$). Thus, across both objects and scenes, representations in scene- and object-selective cortex and hippocampus are more similar during recall than encoding.

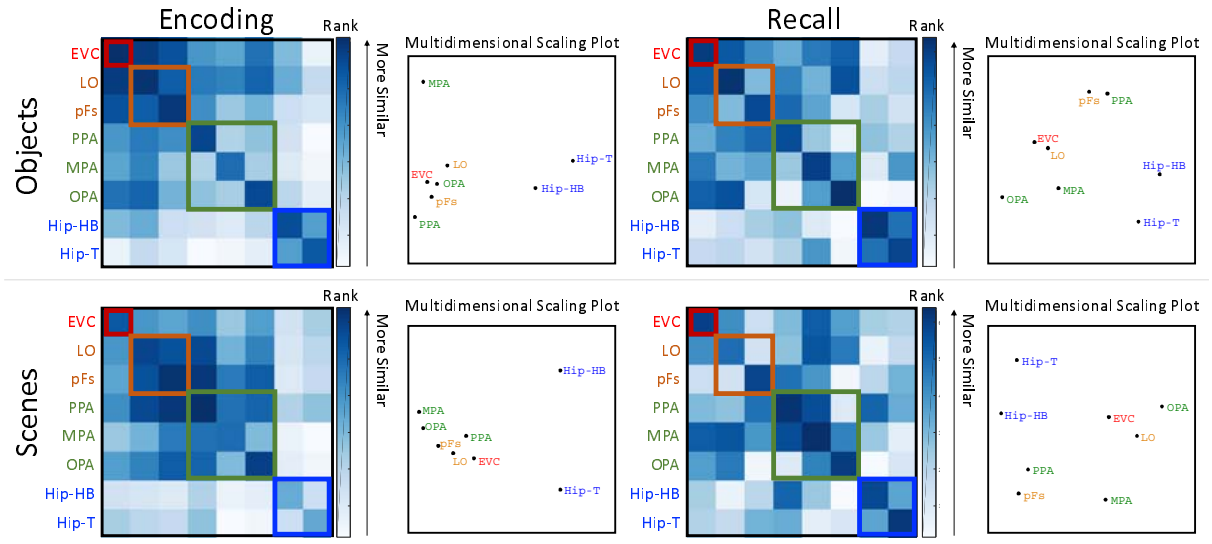

532 **Figure 6 – Comparison of stimulus representations between regions.** Matrices showing Pearson correlations
533 between the RSMs of every ROI pair, using separate halves of the data. Matrices for encoding and recall are shown
534 separately for objects and scenes, and are ranked for visualization purposes. In the matrices, dark blue indicates
535 the most similar ROIs, while white indicates the most dissimilar ROIs. ROIs can be conceptually divided into four
536 groups as indicated by the colored squares – early visual areas (red: EVC), object-selective areas (orange: LO, pFs),
537 scene-selective areas (green: PPA, MPA, OPA), and hippocampus (blue: Hip-HB, Hip-T). Next to the encoding and
538 recall RSMs are multidimensional scaling (MDS) plots, which transform a given RSM into a two-dimensional
539 representation where shorter distances indicate higher similarity. With this, one can visualize which ROIs have
540 similar representations to another. During encoding, while hippocampal regions (blue) are very distinct in their
541 representations from visual regions, they become more similar to visual regions during recall.
542

543 **Direct comparison of encoding and recall discriminability in scene- and object-selective ROIs**
544 **and hippocampus**

545 If we directly compare the ability to discriminate information during encoding and recall,
546 do we find a correlation or an overlap in discriminability? We conducted a discriminability
547 analysis in 3-voxel radius spherical searchlights throughout the scene- and object-selective and
548 hippocampal ROIs to see whether there were differences in which searchlights could best
549 discriminate encoding information versus recall information. Given that these regions only
550 showed discriminability for broad stimulus class (scenes, objects) during recall, we focused on
551 this specific comparison in our searchlight. MPA, LO, pFs, and Hip-HB showed significant
552 correlations between encoding and recall discriminability (MPA: Mean Spearman's rank
553 correlation, ρ=0.121, Wilcoxon signed rank test: Z=2.22, p=0.026; LO: ρ=0.100, Z=2.94, p=0.003;
554 pFs: ρ=0.163, Z=2.26, p=0.024; Hip-HB: ρ=0.070, Z=2.52, p=0.012). Scene-selective regions PPA
555 and OPA did not show a significant correlation between encoding and recall discriminability,

nor did Hip-T (PPA: ρ=0.019, Z=0.18, p=0.858; OPA: ρ=0.020, Z=0.18, p=0.858; Hip-T: ρ=-0.009, Z=-0.41, p=0.685. Thus, we found mixed results—while some regions showed similarities between encoding and recall, others did not.

To investigate this further, we focused on the top 10% of searchlights that showed encoding discriminability and compared their overlap with the top 10% of searchlights that showed recall discriminability within each ROI (Figure 7). If the same voxels perform encoding and recall discrimination, we should find significantly higher overlap than chance. Conversely, if encoding and recall information comprise distinct sets of voxels, we should find lower overlap than chance. PPA and OPA showed significantly lower overlap of these encoding-recall searchlights than a permuted chance level of 10% (PPA: M=4.90%, Wilcoxon rank sum test: Z=3.61, p=3.06 × 10^{-4}; OPA: M=6.74%, Z=3.44, p=5.79 × 10^{-4}). All other regions showed no significantly different overlap than predicted by chance (MPA: M=12.3%; LO: M=14.3%; pFS: M=19.0%; Hip-HB: M=15.9%; Hip-T: M=15.6%; all p > 0.10). Importantly, no region showed significantly higher overlap than chance, indicating that for none of these ROIs were the top voxels for encoding the same as the top voxels for recall.

These results suggest a segregation in late visual cortex between voxels that maintain encoding information and those that maintain recall information.

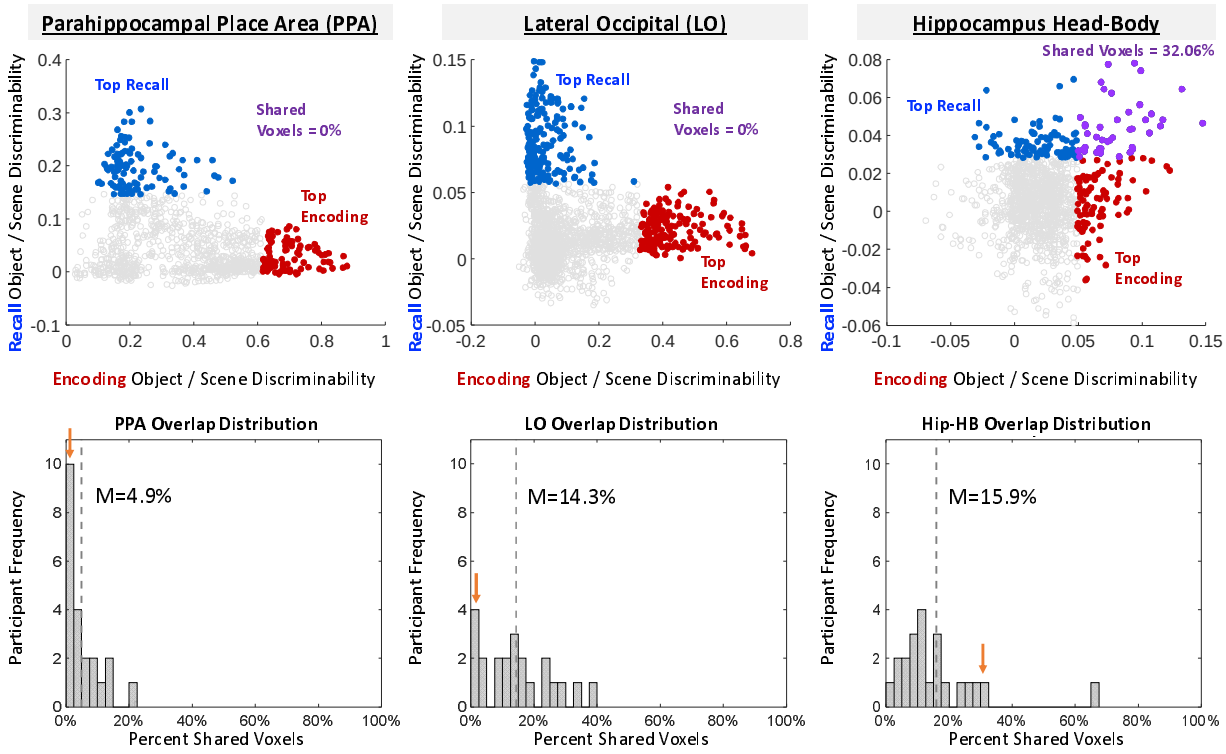

Figure 7 – Comparing encoding and recall discriminability within the ROIs. (a) Example ROIs from a single example participant, where each point represents a voxel-centered spherical searchlight in that ROI and is plotted by the object/scene discrimination index during encoding (x-axis) versus the object/scene discrimination index during recall (y-axis). The top 10% of searchlights showing recall discriminability are colored in blue, while the top 10% of searchlights showing encoding discriminability are colored in red. Searchlights that overlap between the two (those that demonstrate both encoding and recall discrimination) are colored in purple. Note that while the PPA and LO shows no overlap for this participant, Hip-HB show greater overlap. (b) Histograms for these ROIs showing participant distribution of the percentage of overlap between the top 10% of encoding discriminating and top 10% of recall discriminating voxels. The orange arrow represents the participant's data plotted in (a), while the dashed grey line shows the mean overlap percentage. Note that in general, there is low overlap across participants and regions in the top voxels for encoding and those for recall.

Whole-Brain Investigation of Encoding and Recall Effects

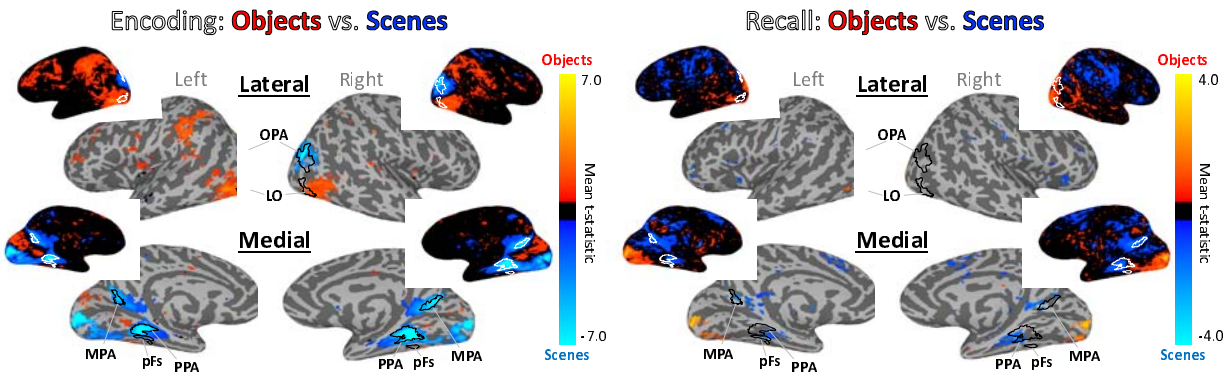

Figure 8 – Whole-brain activation of objects and scenes during encoding and recall. Univariate whole-brain t-statistic maps of the contrast of objects (red/yellow) versus scenes (blue/cyan) in encoding (left) and recall (right). Contrasts show group surface-aligned data (N=22), presented on the SUMA 141-subject standard surface brain (Saad and Reynolds, 2012). Outlined ROIs are defined by voxels shared by at least 25% participants from their individual ROI definitions (using independent functional localizers), with the exception of the pFs and OPA which were defined by 13% overlap (there were no voxels shared by 25% of participants). The encoding maps are thresholded at FDR corrected $q<0.05$. For the recall maps, no voxels passed FDR correction, so the contrast presented is thresholded at $p<0.01$ for visualization purposes. Smaller surface maps show unthresholded results.

Given the differences we observed between encoding and recall within ROIs, we conducted follow-up analyses at the whole-brain level. Looking at a group univariate contrast of objects versus scenes during encoding (Figure 8), we confirm that stimulus class selectivity is strongest in ROIs predicted by the literature: LO and pFs show high sensitivity to objects, while PPA, MPA, and OPA show high sensitivity to scenes (e.g., Epstein and Kanwisher, 1998; Grill-Spector et al., 2001). However, a group univariate contrast of objects versus scenes during recall reveals that recall scene-selectivity is strongest in areas anterior to PPA and MPA, and recall object-selectivity is strongest in areas anterior to LO and in early visual cortex. Rather than the peaks of recalled stimulus class overlapping with those of encoding, the greatest

scene-object differences occur in a spatially separate set of voxels largely anterior to those during encoding.

A searchlight analysis looking at information discriminability across the brain replicates this spatial separation (Figure 9). During encoding, scenes and objects are most discriminable in the same regions identified by the independent perceptual localizer (LO, pFS, PPA, MPA, OPA). However, during recall, peak discriminability occurs in voxels anterior to these regions, especially for the PPA, MPA, and left LO and OPA. Next, we employed a cross-discrimination searchlight to identify regions with shared stimulus representations between encoding and recall. Again, areas anterior to those most sensitive during encoding showed highest similarity between encoding and recall representations.

These results suggest a spatial separation between encoding and recall with strongest reinstatement occurring outside of scene- and object-selective regions typically localized in visual tasks.

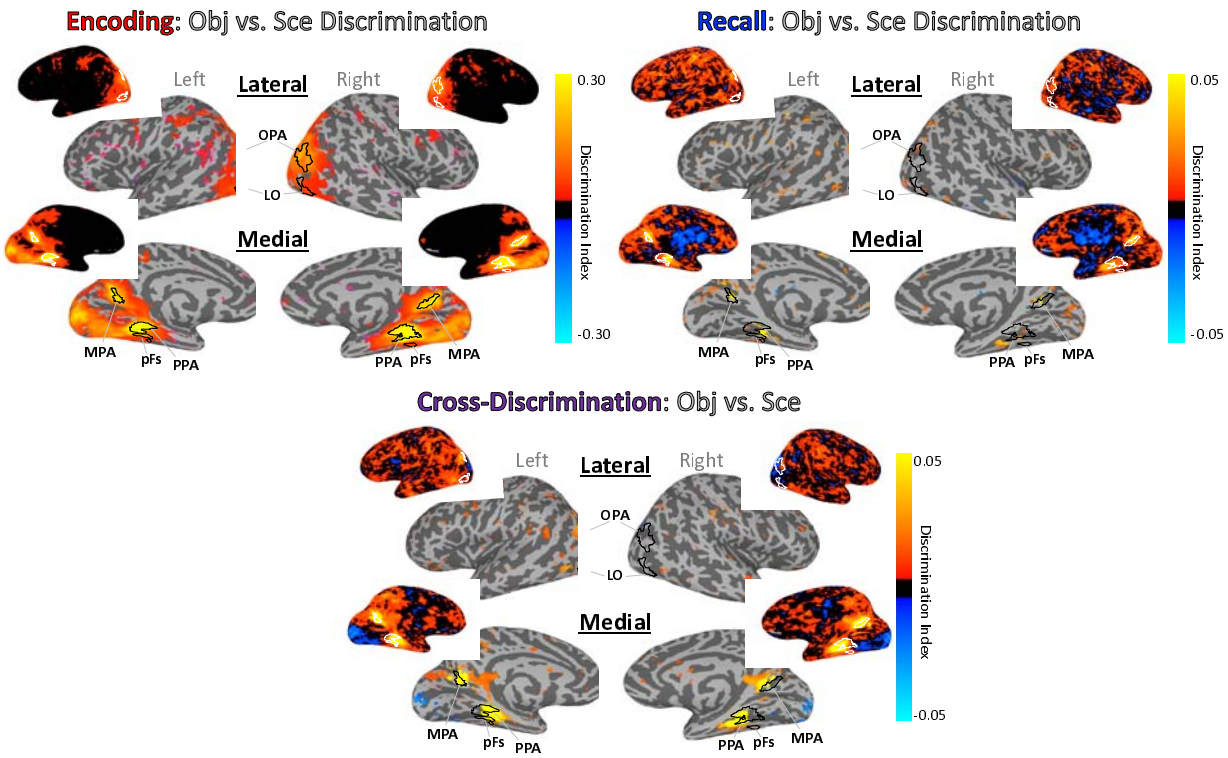

Figure 9 – Whole-brain discrimination analyses for encoding, recall, and cross-decoding of information. Whole-brain searchlight analyses investigating discrimination of objects versus scenes during encoding (top left), recall (top right), and cross-discrimination (bottom). Brighter yellows indicate higher discrimination indices. Outlined ROIs are defined using independent stimuli in an independent localizer run. All maps are thresholded at $p<0.01$ uncorrected, and unthresholded maps are also shown. The cross-discrimination searchlight shows regions that have a shared representation between encoding and recall.

Discussion

In this work, we conducted an in-depth investigation of how and where recalled memory content for complex object and scene images is represented in the brain. First, we observed a striking difference in the granularity of representations in cortex between encoding and recall. While information in cortex during encoding reflected multiple levels of information, during recall we observed clear evidence for coarse level information (objects versus scenes)

637 only. Second, a direct comparison between encoding and recall discriminability within cortical
638 and hippocampal ROIs found mixed results. Further, there was a segregation between the
639 subregions containing the most information during encoding and those during recall. Third,
640 there was an increase in the similarity between hippocampal and cortical regions from
641 encoding to recall. Finally, a whole brain comparison of encoding and recall discriminability
642 revealed that the peaks for recall as well as the strongest encoding-recall similarity were
643 spatially anterior to the peaks during encoding. Collectively, our results reveal key spatial and
644 representational differences between encoding and recalling stimulus content.

645 The ability to decode scenes versus objects during recall is consistent with several
646 findings showing broad stimulus class decodability during recall (Polyn et al., 2005; Reddy et al.,
647 2010; Boccia et al., 2019; O'Craven and Kanwisher, 2000). Additionally, we replicate several
648 findings observing discriminability of different levels of information during perception (e.g.,
649 Mahon et al., 2007; Walther et al., 2009 Kravitz et al., 2011; Park et al., 2011). We also find a
650 significant ability to decode memory vividness and future recognition success from many
651 cortical regions as shown in prior work (Brewer et al., 1998; Wais, 2008; Dijkstra et al., 2017;
652 Fulford et al., 2018). However, at face-value our findings appear to be at odds with prior work
653 that reported fine-grained information during recall as well as encoding-recall similarity in
654 category-selective cortex. We discuss each of these issues in turn in the paragraphs below.

655 In terms of fine-grained information during recall, prior work has reported an ability to
656 decode individual items (Chadwick et al., 2010; Lee et al., 2012; Kuhl and Chun, 2014; Wing et
657 al., 2015; Mack and Preston, 2016; Tompary et al., 2016). However, in these studies, the
658 information decoded could reflect image-specific features and not necessarily a general

representation of the items. In our study, we specifically tested for generalizable stimulus content representations and not individual images, never comparing encoding or recalling an image with itself. Instead, we compared representations across exemplars and focused on stimulus category, to minimize the contribution of image-specific features. The resulting inability to detect fine-grained information during recall suggests that imagery-based representations in scene- and object-selective visual areas may not contain more abstracted or generalized levels of information. Instead, participants may be recalling limited image features, sufficient for image-level classification or classification at the broad level of scenes versus objects (given large differences between their features), but not more abstracted classifications like base-level category (e.g., living room), or properties (e.g., natural or manmade).

In terms of encoding-recall similarity, our results also appear to be inconsistent with some previous findings of sensory reinstatement, in which the neurons or voxels sensitive during encoding have been reported to show the same patterns during recall (Wheeler et al., 2000; Danker and Anderson, 2010; Buchsbaum et al., 2012; Johnson and Johnson, 2014; Schultz et al., 2019). Within scene- and object-selective cortex, we observed limited overlap between the sub-regions with peak encoding and those with peak recall information, with the strongest encoding-recall similarity in more anterior regions. These results are not in conflict with many studies reporting encoding-recall similarity in areas outside of category-selective cortex such as the medial temporal lobe (e.g., Tompary et al., 2016; Schultz et al., 2019). However, some studies do report encoding-recall similarity within scene- and object-selective cortex (e.g., O'Craven and Kanwisher, 2000; Johnson and Johnson, 2014) which may be attributable to key methodological differences from the current study. First, as noted above, we targeted

recollection of stimulus content rather than individual items. While scene- and object-selective regions may maintain item-specific visual information during both encoding and recall, our results suggest a difference in representations during encoding and recall at more generalized levels of information. Second, we employed an item-based recall task, rather than associative tasks commonly used to study recall (e.g., Ganis et al., 2004; Zeidman et al., 2015a; Xiao et al., 2017; Jonker et al., 2018). This allowed us to ensure that information we decoded was not related to other factors such as decoding a cue or association.

Our findings suggest a posterior-anterior gradient within cortical regions, in which recalled representations extend anterior to encoding or perceptual representations. These results agree with recent research showing that regions involved in scene memory are anterior to those involved in scene perception, with the possibility of separate perception and memory networks (Baldassano et al., 2016; Burles et al., 2018; Chrastil, 2018; Silson et al., 2019a). This anterior bias for recall may reflect top-down refreshing of a memory representation in contrast to the largely bottom-up processes that occur during perception (Mechelli et al., 2004; Johnson et al., 2007; Dijkstra et al., 2019). Indeed, recent work using electroencephalography (EEG) has identified a reversal of information flow during object recall as compared to encoding (Linde-Domingo et al., 2019). Alternatively, other research has suggested a gradient within the neocortex that reflects a split of conceptual information represented anterior (or downstream) to perceptual information (Peelen and Caramazza, 2012; Borghesani et al., 2016; Martin, 2016). While recent work shows highly detailed visual content within recalled memories (Bainbridge et al., 2019), it is possible recalled memories may be more abstracted and conceptual compared to their encoded representations. This recalled memory could thus contain less fine-grained

703 perceptual information or be abstracted into a different representation, explaining why we can
704 decode memory strength but not fine-grained perceptually-defined distinctions (e.g., natural
705 versus manmade) during recall. Collectively, our results support these two possible accounts for
706 anterior-posterior gradients of memory/perception or conceptual/perceptual information in
707 the brain, in contrast with other accounts claiming an identical representation between
708 encoding and recall (e.g., Schultz et al., 2019).

709 The current work also provides further support for a content-independent role of the
710 hippocampus in memory. During encoding, we observe broad content selectivity in the
711 hippocampus, as has been observed in other recent work claiming a perceptual role for the
712 hippocampus (Zeidman et al., 2015b; Hodgetts et al., 2017). However, we do not observe
713 strong evidence of any other content representations during encoding or recall; the
714 hippocampus does not show sensitivity to more fine-grained information, and during recall, it
715 does not even show differences at the broadest distinction of objects versus scenes. These
716 results lend support for the notion that the hippocampus is largely content-independent
717 (Davachi, 2006; Danker and Anderson, 2010; Liang et al., 2013; Schultz et al., 2019), with
718 individual item decoding in previous work possibly driven by decoding of indexes within the
719 hippocampus connected to fuller representations in the neocortex, or a coding of memory
720 strength (e.g., Teyler and Rudy, Jonker et al., 2018). In fact, while stimulus content during recall
721 is not discriminable, we find that memory strength is decodable from the hippocampus,
722 mirroring similar results finding strength but not content representations in the hippocampus
723 for oriented gratings (Bosch et al., 2014). There is also evidence to suggest that the
724 hippocampus may require longer delays (e.g., several hours to a week) to develop decodable

representations of memory content (Tompary and Davachi, 2017; Lee et al., 2019), and so a similar experiment conducted with longer delays between study and test (e.g., days) may find decodable stimulus content from the hippocampus.

The current study combining nested categorical structure for real-world images and an item-based recall approach allows us to observe different levels of stimulus representations across the brain; however, there are limitations to this methodology that could be addressed in future work. First, the relative lack of fine-grained information during recall could partly reflect a lack of power that could benefit from a larger stimulus set or a memory task that emphasizes these different stimulus properties. However, it is important to note that we are able to decode memory strength from these regions during both encoding and recall, suggesting that the difference between encoding and recall is not simply a question of power. In fact, the current sample size (N=22) falls in the higher range compared to related studies (e.g., Lee et al., 2012: N=11; Johnson and Johnson, 2014: N=16; Schultz et al., 2019: N=16). Second, while our current methodology allows us to powerfully test stimulus content divorced from memory for individual items, this means we cannot assess discriminability for individual images. Future studies should investigate whether individual item representations are identical between encoding and recall, even if more general content representations are not. Such findings could have meaningful implications on the nature of representations during recall, suggesting the imagery for an individual item is vivid enough to be item-specific, but results in a limited level of abstraction. Finally, it will be important to see whether these newly defined anterior recall regions show more fine-grained representations of stimulus content during recall, and whether there may be region-specific differences (e.g., the MPA in particular has been a key target for

comparisons of scene perception and scene recall; Burles et al., 2018; Chrastil, 2018; Silson et al., 2019b).

Examining item-based recall and representations of memory content in the brain has ultimately unveiled a rather complex, nuanced relationship of encoding and recall, with strongest encoding-recall similarity occurring largely anterior to scene- and object-selective visual cortex. In the study of memory, it is important to examine not only how we remember, but *what* we are remembering, and this study reveals that the way in which this content is manifested may vary greatly between encoding and recall.

Acknowledgements

We thank Adam Steel, Caroline Robertson, and Alexa Tompary for their helpful comments on the manuscript. This research was supported by the Intramural Research Program of the National Institutes of Health (ZIA-MH-002909), under National Institute of Mental Health Clinical Study Protocol 93-M-1070 (NCT00001360).

References

Bainbridge WA, Oliva A. 2015. Interaction envelope: Local spatial representations of objects at all scales in scene-selective regions. *Neuroimage.* 122:408-416.

Bainbridge WA, Hall EH, Baker CI. 2019. Drawings of real-world scenes during free recall reveal detailed object and spatial information in memory. *Nat Commun.* 10:5.

Baldassano C, Esteva A, Fei-Fei L, Beck DM. 2016. Two distinct scene-processing networks connecting vision and memory. *eNeuro*. 3:ENEURO.0178-16.2016.

Beauchamp MS, Martin A. 2007. Grounding object concepts in perception and action: Evidence from fMRI studies of tools. *Cortex*. 43:461-468.

Boccia M, Sulpizio V, Teghil A, Palermo L, Piccardi L, Galati G, Guariglia C. 2019. The dynamic contribution of the high-level visual cortex to imagery and perception. *Hum Brain Mapp.* 40:2449-2463.

Borghesani V, Pedregosa F, Buiatti M, Amaxon A, Eger E, Piazza M. 2016. Word meaning in the ventral visual path: a perceptual to conceptual gradient of semantic coding. *Neuroimage*. 143:128-140.

Bosch SE, Jehee JFM, Fernández G, Doeller CF. 2014. Reinstatement of associative memories in early visual cortex is signaled by the hippocampus. *J Neurosci*. 34:7493-7500.

Brewer JB, Zhao Z, Desmond JE, Glover GH, Gabrieli JDE. 1998. Making memories: Brain activity that predicts how well visual experience will be remembered. *Science*. 281:1185-1187.

Brodt S, Gais S, Beck J, Erb M, Scheffler K, Shönauer M. 2018. Fast track to the neocortex: A memory engram in the posterior parietal cortex. *Science*. 362:1045-1048.

Buckner RL, Wheeler ME. 2001. The cognitive neuroscience of remembering. *Nat Rev Neurosci.* 2:624.

Burles F, Ultimá A, McFarlane LH, Potocki K, Iara G. 2018. Ventral-dorsal functional contribution of the posterior cingulate cortex in human spatial orientation: A meta-analysis. *Front Hum Neurosci*. 12:190.

Buschbaum BR, Lemire-Rodger S, Fang C, Abdi H. 2012. The neural basis of vivid memory is patterned on perception. *J Cogn Neurosci.* 24:1867-1883.

Chadwick MJ, Hassabis D, Weiskopf N, Maguire E. 2010. Decoding individual episodic memory traces in the human hippocampus. *Curr Biol.* 20:544-547.

Chrastil ER. 2018. Hetereogeneity in human retrosplenial cortex: A review of function and connectivity. *Behav Neurosci*. 132:317-338.

Cichy RM, Pantazis D, Oliva A. 2014. Resolving human object recognition in space and time. *Nat Neurosci*. 17:455.

Cox RW. 1996. AFNI: Software for analysis and visualization of functional magnetic resonance neuroimages. *Comput Biomed Res*. 29:162-173.

Danker JF, Anderson JR. 2010. The ghosts of brain states past: Remembering reactivates the brain regions engaged during encoding. *Psychol Bull*. 136:87.

Davachi L, Mitchell JP, Wagner AD. 2003. Multiple routes to memory: Distinct medial temporal lobe processes build item and source memories. *Proc Natl Acad Sci USA*. 100:2157-2162.

Davachi L. 2006. Item, context and relational episodic encoding in humans. *Curr Opin Neurobiol*. 16:693-700.

Dickerson BC, Miller SL, Greve DN, Dale AM, Albert MS, Schacter DL, Sperling RA. 2007. Prefrontal-hippocampal-fusiform activity during encoding predicts intraindividual differences in free recall ability: an event-related functional-anatomic MRI study. *Hippocampus*. 17:1060-1070.

Dijkstra N, Bosch SE, van Gerven MA. 2017. Vividness of visual imagery depends on the neural overlap with perception in visual areas. *J Neurosci*. 37:1367-1373.

Dijkstra N, Bosch SE, van Gerven MAJ. 2019. Shared neural mechanisms of visual perception and imagery. *Trends Cogn Sci*. 23:423-434.

Dilks DD, Julian JB, Paunov AM, Kanwisher N. 2013. The occipital place area is causally and selectively involved in scene perception. *J Neurosci*. 33:1331-1336.

835

836 Epstein R, Kanwisher N. 1998. A cortical representation of the local visual environment. *Nature*.
837 392:598.

838

839 Fulford J, Milton F, Salas D, Smith A, Simler A, Winlove C, Zeman A. 2018. The neural correlates
840 of visual imagery vividness – an fMRI study and literature review. *Cortex*. 105:26-40.

841

842 Ganis G, Thompson WL, Kosslyn SM. 2004. Brain areas underlying visual mental imagery and
843 visual perception: an fMRI study. *Cogn Brain Res*. 20:226-241.

844

845 Gelbard-Sagiv H, Mukamel R, Harel M, Malach R, Fried I. 2008. Internally generated reactivation
846 of single neurons in human hippocampus during free recall. *Science*. 322:96-101.

847

848 Gold JJ, Hopkins RO, Squire LR. 2006. Single-item memory, associative memory, and the human
849 hippocampus. *Learn Mem.* 13:644-649.

850

851 Grèzes J, Tucker M, Armony J, Ellis R, Passingham RE. 2003. Objects automatically potentiate
852 action: an fMRI study of implicit processing. *Eur J Neurosci*. 17:2735-2740.

853

854 Grill-Spector K, Kourtzi Z, Kanwisher N. 2001. The lateral occipital complex and its role in object
855 recognition. *Vis Res*. 41:1409-1422.

856

857 Harel A, Kravitz DJ, Baker CI. 2013. Deconstructing visual scenes in cortex: Gradients of object
858 and spatial layout information. *Cereb Cortex*. 23:947-957.
859
860 Harel A, Kravitz DJ, Baker CI. 2014. Task context impacts visual object processing differentially
861 across the cortex. *Proc Natl Acad Sci USA*. 111:E962-E971.
862
863 Henriksson L, Khaligh-Razavi S-M, Kay K, Kriegeskorte N. 2015. Visual representations are
864 dominated by intrinsic fluctuations correlated between areas. *NeuroImage*. 114:275-286.
865
866 Hodgetts CJ, Voets NL, Thomas AG, Clare S, Lawrence AD, Graham KS. 2017. Ultra-high-field
867 fMRI reveals a role for the subiculum in scene perceptual discrimination. *J Neurosci*. 37:3150-
868 3159.
869
870 Huffman DJ, Stark CE. 2014. Multivariate pattern analysis of the human medial temporal lobe
871 revealed representationally categorical cortex and representationally agnostic hippocampus.
872 *Hippocampus*. 24:1394-1403.
873
874 Iglesias JE, Augustinack JC, Nguyen K, Player CM, Player A, Wright M, Roy N, Frosch MP, McKee
875 AC, Wald LL, Fischl B, van Leemput K. 2016. A computational atlas of the hippocampal
876 formation using ex vivo, ultra-high resolution MRI: Application to adaptive segmentation of in
877 vivo MRI. *Neuroimage*. 115:117-137.
878

879 Ishai A, Ungerleider LG, Haxby JV. 2000. Distributed neural systems for the generation of visual
880 images. *Neuron*. 28:979-990.
881
882 Ison MJ, Quiroga RQ, Fried I. 2015. Rapid encoding of new memories by individual neurons in
883 the human brain. *Neuron*. 87:220-230.
884
885 Johnson MR, Mitchell KJ, Raye CL, D'Esposito M, Johnson MK. 2007. A brief thought can
886 modulate activity in extrastriate visual areas: Top-down effects of refreshing just-seen visual
887 stimuli. *Neuroimage*. 37:290-299.
888
889 Johnson JD, McDuff SG, Rugg MD, Norman KA. 2009. Recollection, familiarity, and cortical
890 reinstatement: A multivoxel pattern analysis. *Neuron*. 63:697-708.
891
892 Johnson MR, Johnson MK. 2014. Decoding individual natural scene representations during
893 perception and imagery. *Front Hum Neurosci*. 8:59.
894
895 Jonker TR, Dimsdale-Zucker H, Ritchey M, Clarke A, Ranganath C. 2018. Neural reactivation in
896 parietal cortex enhances memory for episodically linked information. *Proc Natl Acad Sci USA*.
897 115:11084-11089.
898
899 Kahn I, Davachi L, Wagner AD. 2004. Functional-neuroanatomic correlates of recollection:
900 Implications for models of recognition memory. *J Neurosci*. 24:4172-4180.

901

902 Konkle T, Oliva A. 2012. A real-world size organization of object responses in occipitotemporal

903 cortex. *Neuron*. 74:1114-1124.

904

905 Kravitz DJ, Peng CS, Baker CI. 2011. Real-world scene representations in high-level visual cortex:

906 It's the spaces more than the places. *J Neurosci*. 31:7322-7333.

907

908 Kriegeskorte N, Mur M, Bandettini P. 2008. Representational similarity analysis – connecting

909 the branches of systems neuroscience. *Front Syst Neurosci*. 2:4.

910

911 Kuhl BA, Rissman J, Wagner AD. 2012. Multi-voxel patterns of visual category representation

912 during episodic encoding are predictive of subsequent memory. *Neuropsychologia*. 50:458-469.

913

914 Kuhl BA, Chun MM. 2014. Successful remembering elicits event-specific activity patterns in

915 lateral parietal cortex. *J Neurosci*. 34:8051-8060.

916

917 LaRocque KF, Smith ME, Carr VA, Witthoft N, Grill-Spector K, Wagner AD. 2013. Global similarity

918 and pattern separation in the human medial temporal lobe predict subsequent memory. *J*

919 *Neurosci*. 33:5466-5474.

920

921 Lee SH, Kravitz DJ, Baker CI. 2012. Disentangling visual imagery and perception of real-world

922 objects. *Neuroimage*. 59:4064-4073.

923

924 Lee SH, Kravitz DJ, Baker CI. 2019. Differential representations of perceived and retrieved visual
925 information in hippocampus and cortex. *Cereb Cortex*. 29:4452-4461.

926

927 Lewis JW. 2006. Cortical networks related to human use of tools. *Neuroscientist*. 12:211-231.

928

929 Liang JC, Wagner AD, Preston AR. 2013. Content representation in the human medial temporal
930 lobe. *Cereb Cortex*. 23:80-96.

931

932 Linde-Domingo J, Treder, MS, Kerrén C, Wimber M. 2019. Evidence that neural information flow
933 is reversed between object perception and object reconstruction from memory. *Nat Commun*.
934 10:179.

935

936 Mack ML, Preston AR. 2016. Decisions about the past are guided by reinstatement of specific
937 memories in the hippocampus and perirhinal cortex. *Neuroimage*. 127:144-157.

938

939 Mahon BZ, Milleville SSC, Negri GAL, Rumiati RI, Caramazza A, Martin A. 2007. Action-related
940 properties shape object representations in the ventral stream. *Neuron*. 55:507-520.

941

942 Martin A. 2016. GRAPES—Grounding representations in action, perception, and emotion
943 systems: How object properties and categories are represented in the human brain. *Psychon*
944 *Bull Rev*. 23:979-990.

McClelland JL, McNaughton BL, O'Reilly RC. 1995. Why there are complementary learning systems in the hippocampus and neocortex: Insights from the successes and failures of connectionist models of learning and memory. *Psychol Rev*. 102:419.

Mechelli A, Price CJ, Friston KJ, Ishai A. 2004. Where bottom-up meets top-down: Neuronal interactions during perception and imagery. *Cereb Cortex*. 14:1256-1265.

O'Craven KM, Kanwisher N. 2000. Mental imagery of faces and places activates corresponding stimulus-specific brain regions. *J Cogn Neurosci*. 12:1013-1023.

Park S, Brady TF, Greene MR, Oliva A. 2011. Disentangling scene content from spatial boundary: Complementary roles for the parahippocampal place area and lateral occipital complex in representing real-world scenes. *J Neurosci*. 31:1333-1340.

Peelen MV, Caramazza A. 2012. Conceptual object representations in human anterior temporal cortex. *J Neurosci*. 32:15728-15736.

Polyn SM, Natu VS, Cohen JD, Norman KA. 2005. Category-specific cortical activity precedes retrieval during memory search. *Science*. 310:1963-1966.

966 Ranganath C, Ritchey M. 2012. Two cortical systems for memory-guided behavior. *Nat Rev*
967 *Neurosci*. 13:713-726.
968
969 Reddy L, Tsuchiya N, Serre T. 2010. Reading the mind's eye: Decoding category information
970 during mental imagery. *Neuroimage*. 50:818-825.
971
972 Ritchey M, Wing EA, LaBar KS, Cabeza R. 2013. Neural similarity between encoding and retrieval
973 is related to memory via hippocampal interactions. *Cereb Cortex*. 23:2818-2828.
974
975 Ross DA, Sadil P, Wilson DM, Cowell RA. 2017. Hippocampal engagement during recall depends
976 on memory content. *Cereb Cortex*. 28:2685-2698.
977
978 Rugg MD, King DR. 2018. Ventral lateral parietal cortex and episodic memory retrieval. *Cortex*.
979 107:238-250.
980
981 Saad ZS, Reynolds RC. 2012. SUMA. *Neuroimage*. 62:768-773.
982
983 Schultz H, Tibon R, LaRocque KF, Gagnon SA, Wagner AD, Staresina BP. 2019. Content tuning in
984 the medial temporal lobe cortex: Voxels that perceive, retrieve. *eNeuro*. 6.
985
986 Silson EH, Steel AD, Baker, CI. 2016. Scene-selectivity and retinotopy in medial parietal cortex.
987 *Front Hum Neurosci*. 10:412.

988

989 Silson EH, Steel A, Kidder A, Gilmore AW, Baker CI. 2019a. Distinct subdivisions of human
990 medial parietal cortex support recollection of people and places. *eLife*. 8.
991

992 Silson EH, Gilmore AW, Kalinowski SE, Steel A, Kidder A, Martin A, Baker, CI. 2019b. A posterior-
993 anterior distinction between scene perception and scene construction in human medial parietal
994 cortex. *J Neurosci*. 39:705-717.
995

996 Staresina BP, Davachi L. 2006. Differential encoding mechanisms for subsequent associative
997 recognition and free recall. *J Neurosci*. 26:9162-9172.
998

999 Staresina BP, Henson RN, Kriegeskorte N, Alink A. 2012. Episodic reinstatement in the medial
1000 temporal lobe. *J Neurosci*. 32:18150-18156.
1001

1002 Sullivan Giovanello K, Schnyer DM, Verfaellie M. 2003. A critical role for the anterior
1003 hippocampus in relational memory: Evidence from an fMRI study comparing associative and
1004 item recognition. *Hippocampus*. 14:5-8.
1005

1006 Teyler TJ, Rudy JW. 2007. The hippocampal indexing theory and episodic memory: Updating the
1007 index. *Hippocampus*. 17:1158-1169.
1008

1009 Tompary A, Davachi L. 2017. Consolidation promotes the emergence of representational
1010 overlap in the hippocampus and medial prefrontal cortex. *Neuron.* 96:228-241.
1011
1012 Tompary A, Duncan K, Davachi L. 2016. High-resolution investigation of memory-specific
1013 reinstatement in the hippocampus and perirhinal cortex. *Hippocampus.* 26:995-1007.
1014
1015 Troiani V, Stigliani A, Smith ME, Epstein RA. 2012. Multiple object properties drive scene-
1016 selective regions. *Cereb Cortex.* 24:883-897.
1017
1018 Valyear KF, Cavina-Pratesi C, Stiglick AJ, Culham J. 2007. Does tool-related fMRI activity within
1019 the intraparietal sulcus reflect the plan to grasp? *Neuroimage.* 36:T94-T108.
1020
1021 Vilberg KL, Rugg MD. 2009. Functional significance of retrieval-related activity in lateral parietal
1022 cortex: Evidence from fMRI and ERPs. *Hum Brain Map*. 30:1490-1501.
1023
1024 Wais PE. 2008. fMRI signals associated with memory strength in the medial temporal lobes: A
1025 meta-analysis. *Neuropsychologia.* 46:3185-3196.
1026
1027 Walther DB, Caddigan E, Fei-Fei L, Beck DM. 2009. Natural scene categories revealed in
1028 distributed patterns of activity in the human brain. *J Neurosci*. 29:10573-10581.
1029

1030 Wheeler ME, Petersen SE, Buckner RL. 2000. Memory's echo: Vivid remembering reactivates
1031 sensory-specific cortex. *Proc Natl Acad Sci USA*. 97:11125-11129.
1032
1033 Wing EA, Ritchey M, Cabeza R. 2015. Reinstatement of individual past events revealed by the
1034 similarity of distributed activation patterns during encoding and retrieval. *J Cogn Neurosci.*
1035 27:679-691.
1036
1037 Xiao X, Dong Q, Gao J, Men W, Poldrack R, Xue G. 2017. Transformed neural pattern
1038 reinstatement during episodic memory retrieval. *J Neurosci*. 37:2986-2998.
1039
1040 Zeidman P, Lutti A, Maguire EA. 2015a. Investigating the functions of subregions within anterior
1041 hippocampus. *Cortex*. 73:240-256.
1042
1043 Zeidman P, Mullally SL, Maguire EA. 2015b. Constructing, perceiving, and maintaining scenes:
1044 hippocampal activity and connectivity. *Cereb Cortex*. 252:3836-3855.
1045
1046 Zeineh MM, Engel SA, Thompson PM, Bookheimer SY. 2003. Dynamics of the hippocampus
1047 during encoding and retrieval of face-name pairs. *Science*. 299:577-580.